

Synthesis of cellulosic wastepaper modified biobased superabsorbent hydrogel composite

Highlights

This chapter presents the fabrication of superabsorbent hydrogel composites (SAHCs) of starch, itaconic acid, and acrylic acid-based hydrogel with wastepaper-derived cellulosic paper powder as the micro-reinforcing agent. Here, the characterization of the cellulosic paper powder as well as the obtained SAHCs was performed using different analytical, microscopic and spectroscopic techniques. Further, by varying the amounts of the micro-reinforcing agent, its effect on the water absorption capacity (WAC) of the SAHCs was investigated. In addition, SAHC with a high WAC was chosen for NPK fertilizer release and okra seed germination studies. Moreover, the release study was explained by using different kinetic models. Further, a soil burial test was conducted, indicating the biodegradable nature of the hydrogel.

Parts of this chapter are published as

[1] Bora, A., Sarmah, D., and Karak, N. Cellulosic wastepaper modified starch/itaconic acid/acrylic acid-based biodegradable hydrogel as a sustain release of NPK fertilizer vehicle for agricultural applications. *International Journal of Biological Macromolecules*, 253(1):126555, 2023.

3.1. Introduction

As discussed in **Chapter 2**, controlling nutrient loss is considered as a global challenge for the agricultural sector in these days. Since, nutrient deficiency along with poor water content is the major factor limiting agricultural production in arid and semi-arid regions, therefore, improving the utilization of nutrients and water uptake in these areas is of great importance [1,2]. In this sense, sustained/slow-release fertilizer (SRF) could be used as a promising strategy to reduce fertilizer loss, improve efficiency of use, and combat leaching pollution. SRF is the most promising material that contains both fertilizer and hydrogel in the same formulation, releasing nutrients as well as water more sustainably into the environment compared to conventional fertilizers [3]. Further, the use of these materials, minimizes the evaporation loss and irrigation frequency, enhances the water availability and plant growth rate. In this regard, superabsorbent hydrogels (SAHs) as SRF system are being explored as potential material in the agricultural field, which are also used as water holding materials as well as soil conditioners. As described in **Chapter 1**, SAHs are three-dimensional network structure containing hydrophilic polymer chains with a capacity to hold large amounts of water and water-soluble substances within their network structure and released the loaded-fertilizer in a controlled manner, providing sufficient nutrients as well as moisture for the growth of the plants in arid/semi-arid farmlands [4,5]. So far, various polysaccharides-based hydrogels have been developed as SRF vehicles to provide nutrients in a controlled manner to the plants during their growing seasons. For instance, Bauli *et al.* developed carboxymethyl cellulose based hydrogel with citric acid as a cross-linker for sustained release of nitrogen (N), phosphorous (P), and potassium (K) (NPK) fertilizers [6]. Further, they tested the prepared hydrogel for cucumber cultivation. These biobased hydrogels have received much attention due to their biocompatibility, abundancy, biodegradability, and low production costs. Such biobased carriers may also inhibit the generation of environmental pollution due to their biodegradable property, leading to the widespread use of degradable SRF formulations in agriculture.

Besides SAH, production of SAH composite (SAHC) with the incorporation of modifying agents is an efficient strategy to improve properties of SRF systems [7,8]. Therefore, development of SAHCs has attracted a great interest to the researchers in this field. The recent studies have focused on the application of the novel and eco-friendly reinforcing agents to produce economical and efficient SRF composites. Considering this

point, cellulosic materials obtained from waste products, could suppose as a feasible and scalable modifying agent for a hydrogel due to its easily available, inexpensive, and biodegradable properties [9,10]. Among the various solid wastes, wastepaper (WP) is one of the most generated waste materials in our daily life. WP as a biogenic material is a potential raw material source for production and utilization of cellulose as modifying agent and matrix in the preparation of polymeric composites. Papers used for printing newspapers, magazines, office work, packaging and academic purposes are discarded or burned, but very little amount is reutilized [11,12]. Therefore, processing WP into cellulose-based reinforcements and matrices may provide an alternative to paper recycling, addressing the problem of by-products generated in the papermaking process and daily operations [13,14]. Furthermore, they act as both reinforcing agent and physical cross-linker through physical interactions between functional groups of the hydrogel matrix and surface of cellulosic materials. Therefore, the use of cellulosic modifying agent incorporated SRF hydrogel may show eco-friendly and economic win-to-win effects as it reduces fertilizer losses and increases water absorption capacity (WAC) of hydrogel matrix [15,16].

In this work, WP powder (WPP) introduced starch/ itaconic acid (IA)/acrylic acid (AA) based hydrogel was prepared, authenticated, and utilized as SRF system for release of NPK fertilizer. The main objective of using WPP as modifying agent is to enhance the biodegradability and reduce the amounts of synthetic monomers used in the synthesized hydrogel. The use of WP instead of toxic chemicals in the chemical reactions and even as modifying agent is more advantageous from green chemistry point of view. This practice helps to carry out the chemical reaction by using biobased feedstocks which are not only cheap but also non-toxic and renewable. Most importantly, in such applications, WP obtained from cartons, or any other sources can also be used. Thus, this work paves the most useful way for utilization of WP in addition to the others. Further, WAC of the prepared composites were determined as well as fertilizer release kinetics were studied using different kinetic models. Additionally, biodegradability and okra seed (*Abelmoschus esculentus*) germination were investigated to highlight the potential of the prepared hydrogel composites for agricultural applications.

3.2. Experimental section

3.2.1. Materials

Various chemicals including starch, IA, AA, ammonium persulfate (APS), N,N'-methylene bis-acrylamide (MBA), and NaOH were used with similar quality and specifications as mentioned in **Chapter 2**. Further, okra seeds of the same quality are used as those used in the previous chapter.

Printing WPs were acquired from our own laboratory and used as raw material to obtain cellulosic micro-reinforcing agent. The chemical constituent (such as cellulose content, ash, etc.) of the WP was evaluated by solvent extraction using the method described by Mansor *et al.* [17]. It was found that used WP is mainly composed of 75.7% of cellulose, 13.9% of hemicellulose, 5.4% of lignin, 5% of extractives and 18.4% of ash.

Potassium dihydrogen phosphate (KH_2PO_4) as phosphorous standard and ammonium sulphate ($(\text{NH}_4)_2\text{SO}_4$) as nitrogen standard were used for fertilizer release experiment and they were purchased from Merck, India. These two salts are soluble in water. KH_2PO_4 has a molecular weight of 136.08 g/mol and $(\text{NH}_4)_2\text{SO}_4$ has a molecular weight of 132.14 g/mol.

Ammonium molybdate, ascorbic acid, salicylic acid, sodium citrate, sodium nitroprusside, and sodium hypochlorite are coloring reagents used to analyze nitrogen and phosphate content in NPK fertilizer release tests. Ascorbic acid (molecular weight 176.12 g/mol) and salicylic acid (molecular weight 138.12 g/mol) were purchased from SRL, India. Ammonium molybdate has molecular weight of 196.01 g/mol and provided by Thermo Fisher Scientific India Pvt. Ltd. Sodium citrate (molecular weight 258.06 g/mol), sodium nitroprusside (molecular weight 261.92 g/mol) and sodium hypochlorite (molecular weight 74.44 g/mol) were provided by Merck, India. All these chemicals were used without further purifying them.

3.2.2. Methods

3.2.2.1. Methodology used to produce wastepaper powder (WPP)

In order to produce WPP, WPs were cut into small pieces and thoroughly washed by soaking in water for 3-4 h to remove foreign particles and other contaminants. The pulp slurry thus obtained was squeezed to remove water which was further dried in an oven. Thereafter, the dried pulps were grounded using a domestic mixture grinder. This grounded paper (1g) was taken in a 250 mL round bottom flask and 30 mL of 2% (Wt/Vol) solution of NaOH was added into it [18]. Thereafter, mixture was stirred using a mechanical stirrer at 50 °C for 2.5 h. The obtained residue was washed up to a neutral pH and centrifuged to collect the residue which were dried in an oven at 100 °C. Finally,

the oven dried residue was ground into powder using mortar and pestle which was used for further characterization and preparation of the hydrogel composites.

3.2.2.2. Preparation of SAHCs

In this study, SAHCs were fabricated using the best formulation from **Chapter 2** with the additional incorporation of WP-derived cellulosic paper powder as the micro-reinforcing agent. The preparation method involves the same procedure as described in **Chapter 2** with some modifications. To prepare SAHCs, WPP was sonicated for 5 min in 10 mL of 0.067N NaOH solution. After that, appropriate amount of starch and IA was mixed with WPP suspension in a 250 mL three neck RB flask. The mixture was then stirred at 70 °C using a mechanical stirrer. After 10 min of stirring, the reaction mixture was heated again up to 80-85 °C with the addition of AA (with 1 mL of water) to get it a gelatinized texture. Thereafter, a solution of APS and MBA with 1 mL of water was added to initiate the polymerization under nitrogen environment by maintaining the temperature at 70 °C. The reaction was stopped after the formation of a solid mass which was further neutralized with 1.7 mL of 8 N NaOH. The hydrogel product obtained was then allowed to swell in an excess amount of water which was further washed with methanol and dried in an oven at 70 °C. Finally, the oven dried hydrogel was ground into powder and used for further studies. For comparison purpose, a neat hydrogel was also prepared without incorporation of WPP by using the same method as described above.

Table 3.1. SAHCs with various compositions.

Hydrogel	Starch (g)	AA (g)	IA (g)	NPK (g)	WPP (wt%)	MBA (g)	APS (g)
HC	1	0.9	0.1	0	0	0.01	0.04
HC/WPP/0.01	1	0.9	0.1	0	0.01	0.01	0.04
HC/WPP/0.05	1	0.9	0.1	0	0.05	0.01	0.04
HC/WPP/0.1	1	0.9	0.1	0	0.1	0.01	0.04
HC/WPP/5	1	0.9	0.1	0	5	0.01	0.04
HC/WPP/10	1	0.9	0.1	0	10	0.01	0.04
HC/WPP/NPK	1	0.9	0.1	1	0.05	0.01	0.04

3.2.2.3. Preparation of NPK encapsulated SAHCs

The NPK encapsulated hydrogel composite was prepared similarly, except the addition of required amount of NPK fertilizer in it. Furthermore, the NPK fertilizer was added in the first step with starch and IA. The resulting gel-like solid was cut into small pieces and subject to drying in an oven at 60-70 °C for studying the fertilizer release profile and

seed germination of okra. In **Table 3.1**, formulations for the prepared hydrogels are provided.

3.2.2.4. Structural analysis

Chemical analysis of WPP and WPP reinforced hydrogels was carried out by using various analytical, microscopic and spectroscopic techniques. Details of FTIR, TGA and SEM instruments are the same as mentioned in **Chapter 2**. The XRD pattern of the WPP and dried hydrogel composites were characterized by D8 Focus XRD machine (Bruker AXS, Germany) with a scanning rate of 0.1°/min. The morphological study of the hydrogel composites was analyzed through Field emission scanning electron microscopy (FESEM) instrument (JSM-7200 F, Japan). UV spectrophotometer (Thermo Fisher, Model Evolution 300, USA) and Atomic absorption spectrophotometer (AAS) (Thermo Scientific, AAS-ICE 3500, UK) were used to study the controlled release of NPK fertilizers.

3.2.2.5. Swelling test

The maximum WAC (Q_{max}) of the prepared hydrogel composites in distilled water was determined according to **Eq. 2.1** of **Chapter 2**, and the method used was the same as described in **Chapter 2**.

3.2.2.6. Fertilizer (NPK) release experimentation

In order to understand the NPK release behavior of the prepared SAHC, we performed a slow-release experiment using HC/WPP/NPK formulation in distilled water. Briefly, hydrogel was submerged in 100 mL of deionized water. After a predetermined length of time, a required amount of supernatant liquid was withdrawn and used to determine the amount of nutrient N, P and K released into the system. Subsequently, an equal amount of water was added back into the system to keep the release volume constant. The released amount of N and P was determined UV-spectrophotometrically, whereas K was determined by using AAS.

At a wavelength of 855 nm, a UV-Vis spectrophotometer was used to measure the amount of P released [19-21]. For this purpose, 1 mL of supernatant solution was taken and diluted it to 100 times in water. Then, about 2 mL of prepared sample was mixed with 0.8 mL of ascorbic acid and 0.4 mL of ammonium molybdate solution. The absorbance of the resulting blue colored phosphomolybdate complex was measured within 30 min of preparing the sample. Moreover, the amount of N released was also

measured using a UV-spectrophotometer at 695 nm [7,22]. Firstly, 1 mL of aliquot was diluted 100 times. From this solution, 2 mL of diluted hydrogel composite was mixed with 1 mL of each salicylic acid (SA), sodium nitroprusside and sodium hypochlorite solution. Finally, the absorbance of the mixture was recorded, and the amount of N released was determined. To establish a standard curve for determination of concentration of P and N, respectively, the absorbance of a standard solution of potassium dihydrogen phosphate and ammonium sulphate was measured. Moreover, the amount of K released was estimated by diluting 1 mL of supernatant up to 10 times before measuring concentration with AAS. The release studies for all three elements were conducted for up to 20 days. The NPK loading efficiency was calculated using the method described in **Chapter 2**. The cumulative release (%) for each element was calculated using **Eq 2.10** of **Chapter 2**.

3.2.2.7. Kinetic models

To investigate the fertilizer release profile from HC/WPP/NPK formulation in water, the release data obtained through experiment were fitted into the following mathematical models.

- (a) Zero order release kinetic model, represented as-

$$Q_t = Q_{eq} + k_0 t \text{ -----(Eq. 3.1)}$$

- (b) First order release kinetic model, represented as-

$$\log(Q_e - Q_t) = \frac{k_1}{2.303t} + \log Q_e \text{ -----(Eq. 3.2)}$$

- (c) Higuchi model, be written as-

$$Q_t = K_H t^{1/2} \text{ -----(Eq. 3.3)}$$

- (d) Korsmeyer–Peppas model, described as-

$$\frac{Q_t}{Q_{eq}} = K_p t^n \text{ -----(Eq. 3.4)}$$

where Q_t and Q_{eq} denote the quantity of nutrients released at time t and at a state of equilibrium, respectively, whereas K_0 , K_1 , K_H and K_P represents the rate constant of the zero-order, first-order, Higuchi model and Korsmeyer-Peppas model, respectively and n denotes the index of diffusion [17].

3.2.2.8. Biodegradation test

A soil burial test was conducted to observe the biodegradability of HC/WPP/NPK formulation by following the same method as described in **Chapter 2**. However, in this case, fifteen samples were prepared for degradation and the test was carried out for 75 days. In every 15 days, three samples were taken out of the soil and rate of degradation was calculated using **Eq. 2.11** of **Chapter 2**. Moreover, the experiment was evaluated for any changes in chemical structure during biodegradation using FTIR spectroscopic and morphological studies.

3.2.2.9. Seed germination test

In order to study the effect of the HC/WPP/NPK on seed germination rate, root length (RL) and shoot length (SL) of okra seeds, a germination test was performed. For this purpose, seeds of similar sizes were taken, and the test was carried out using two different soils (loam soil and sandy soil) separately as the growth media. Initially, 0.5 g of hydrogel (with and without NPK) was soaked in distilled water and used to observe their effects on germination rate of the seeds. Thereafter, 40 g of soil was placed into a paper cup and swollen hydrogel composites were buried inside the cup with one okra seed placed 1 cm away from the top layer. The test was carried out under three different conditions by placing sample cups outside the lab under the exposure of sunlight and five replicates for each condition was prepared in the case of loam soil (four replicates for each condition were prepared in case of sandy soil). As the first condition, each cup was prepared without any hydrogel, which was coded as Control-1. Cups containing hydrogel composite without NPK were used as the second condition (coded as Control-2) and the third condition was cups containing HC/WPP/NPK. The experiment was conducted without introduction of externally supplied water. For all soil samples, the germination percentage was recorded daily up to the seventh day. A seed was considered as germinated when a radicle of 1–2 mm had grown out of the seed. The germination rate was determined by using **Eq. 2.16** of **Chapter 2**.

3.2.2.10. Statistical analysis

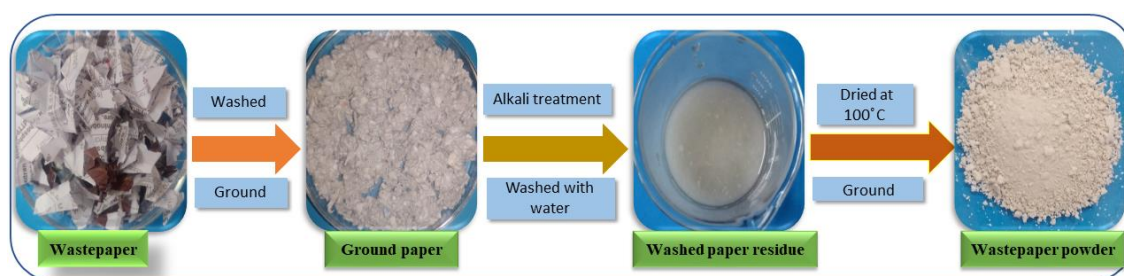
One-way ANOVA was used to analyze statistical data, using the Origin pro software version 8.5. Each measurement was analyzed at least thrice. The results are shown as the average value with standard deviation.

3.3. Results and discussion

3.3.1. Production of wastepaper powder (WPP)

Scheme 3.1. illustrates the flow chart of preparation of WPP from WP and the chemical constituents of raw WP indicate that though WP is one of the most underutilized sources

of cellulosic material, cellulose fibers obtain from this source can serve as the primary reinforcing component. Therefore, this study is envisioned to produce cellulosic WPP from this waste material using simply alkaline treatment. This treatment was applied to remove printing ink and remaining lignin from the WP to get WPP. de Souza *et al.* also reported that alkaline treatment is more appropriate for isolation of cellulosic materials from paper waste [19].



Scheme 3.1. Production of alkali-treated WPP.

3.3.2. Preparation of HC/WPP and HC/WPP/NPK

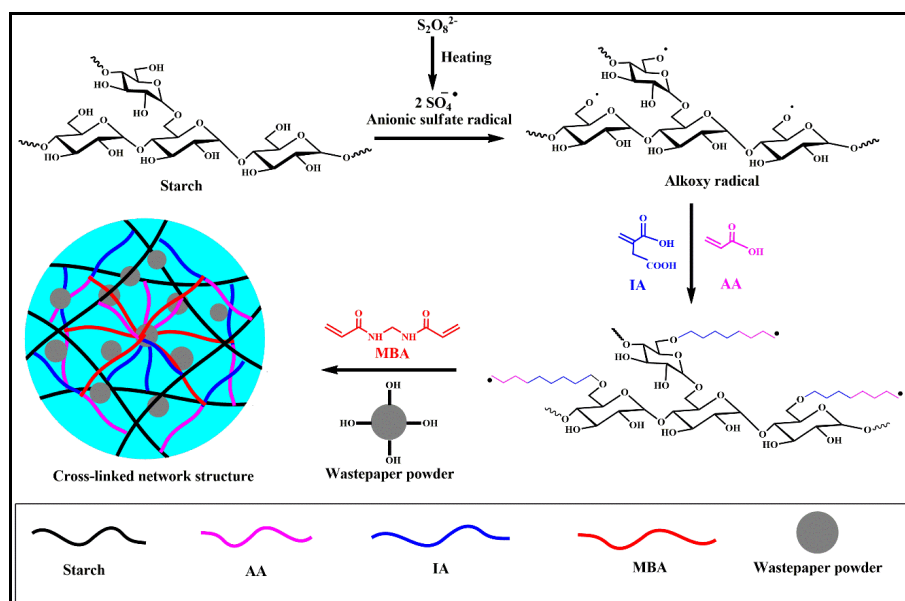
The proposed mechanism of synthesis of WPP incorporated hydrogel was presented in **Scheme 3.2**. Initially, anionic sulphate radicals were generated from APS by thermal dissociation. Then, the generated radicals carried out abstraction of hydrogen from primary hydroxyl group of starch, resulting in the formation of alkoxy macroradicals. Consequently, these macroradicals initiate polymerization at vinyl groups of the monomers (AA and IA) for chains propagation. Moreover, the two end vinyl groups of MBA react simultaneously with the multiple polymer chains leading to the formation of three-dimensionally cross-linked network structures of the hydrogel. Further, the existence of various physical interactions between WPP and the polymer network were observed through different spectroscopic analyses as discussed in later sections [23,24].

3.3.3. Characterization

3.3.3.1. FTIR

The FTIR spectral studies were carried out to understand the chemical structure of WPP, HC and HC/WPP/0.05. The spectra are shown in **Figure 3.1.a**. According to the FTIR spectrum of WPP, the hydrophilicity of cellulosic WPP can be assumed from the band appearing at around 3402 cm^{-1} which can be ascribed to the O-H stretching frequency of hydroxyl groups, whereas C-H and C-O-C stretching frequencies of the β -glycosidic units are represented by bands at approximately 2906 and 1036 cm^{-1} . The peak appeared at 1631 cm^{-1} in the WPP spectrum is ascribed to the O-H bending of adsorbed water [25]. The low-intensity peak in the region $1702\text{--}1731\text{ cm}^{-1}$ for WPP indicates the presence of

other compounds rich in lignin, and hemicellulose. This is indicative of the fact that most of the content of WPP is cellulosic in nature.



Scheme 3.2. Possible mechanism of preparation of WPP incorporated SAHC.

Further, the characteristic peaks from FTIR spectrum of hydrogels with and without WPP, represent the interaction between starch, AA, IA and WPP. A peak related to the stretching vibration of the glycosidic C-O-C linkages present in the starch backbone appeared at 1020 cm^{-1} . Furthermore, the band appeared around 1715 cm^{-1} indicating the stretching vibration of C=O in carboxylate groups of AA and IA. Moreover, the absorption bands at 2921 and 3425 cm^{-1} can be ascribed to the C-H stretching frequencies of CH_2 groups and O-H stretching vibrations of -OH groups, which are the important bands for starch, IA, and AA moiety [26]. Furthermore, the peak around 3425 cm^{-1} in the FTIR spectrum of HC/WPP/0.05 is broadened compared to that of HC which may be due to the presence of strong hydrogen bonding between the hydrogen atom of the -OH group of WPP and the carboxylate group of hydrogel matrix. It indicates the presence of interaction between the modifying agent and the hydrogel matrix.

From the FTIR spectrum of HC/WPP/NPK, which is shown in **Figure 3.1.b**, the absorption peaks appeared around 3432 , 2920 , 1720 and 1020 cm^{-1} belong to the stretching vibrations of O-H, C-H, C=O and C-O-C, respectively, and are typical characteristic peaks of starch, AA and IA, indicating a successful grafting of AA and IA on the starch backbone in the case of HC/WPP/NP [26]. Furthermore, the FTIR spectrum of pure NPK shows peaks around 3463 , 2808 , 1448 and 1151 cm^{-1} which are attributed

to the stretching modes of the NH, O-H, P=O, and P-OH groups, respectively [27]. The FTIR spectrum of HC/WPP/NPK also shows the characteristic peaks associated with NPK. Consequently, it can be concluded that the hydrogel network was successfully loaded with NPK fertilizer.

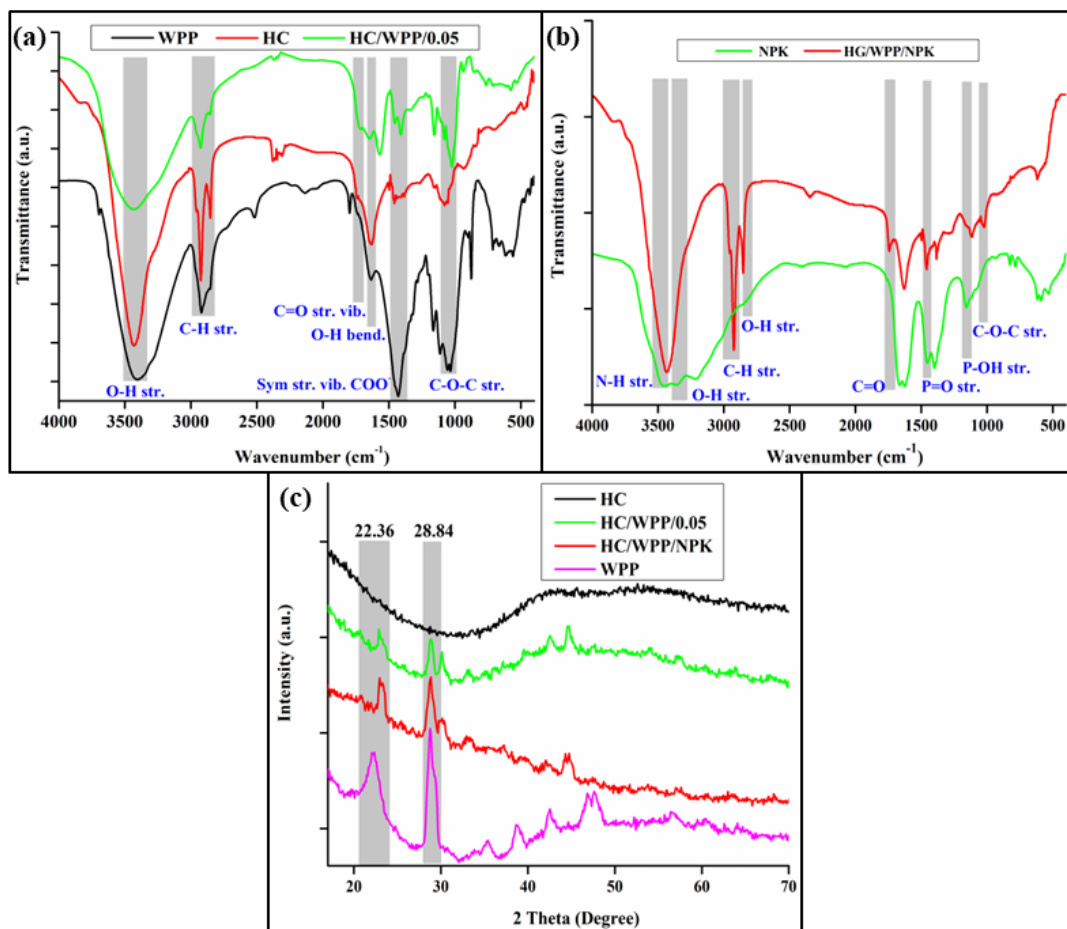


Figure 3.1. FTIR spectra of (a) WPP, HC and HC/WPP/0.05; (b) NPK and HC/WPP/NPK; and (c) XRD pattern of WPP, HC, HC/WPP/0.05 and HC/WPP/NPK.

3.3.3.2. XRD

XRD is a commonly used technique for evaluating the structure and crystallinity of polymer materials [28]. The XRD patterns of alkali-treated WPP, HC, HC/WPP/0.05, and HC/WPP/NPK are shown in **Figure 3.1.c**. From the figure, it is seen that, the characteristic peaks for cellulosic agent were observed around 22 and 29°. Similar peaks were also observed in case of HC/WPP/0.05 and HC/WPP/NPK. However, these peaks were absent in case of HC which indicates the successful introduction of WPP particles in the composite networks.

3.3.3.3. FESEM

Figure 3.2.a illustrates the surface morphology of the WPP, which presents an anisotropic microstructure with granular shape particles. They have a wide range of sizes, with expected average diameters and lengths less than $1\ \mu\text{m}$. Moreover, a magnified FESEM image revealed the porous structure of HC/WPP/0.05 and the interfacial attachment of granular particles on the surface of the polymer matrix (**Figure 3.2.b**). Incorporation of WPP creates a rougher and more porous surface, which favorably influences the diffusion of water into the polymer network, leading to increased water absorption capacity [28].

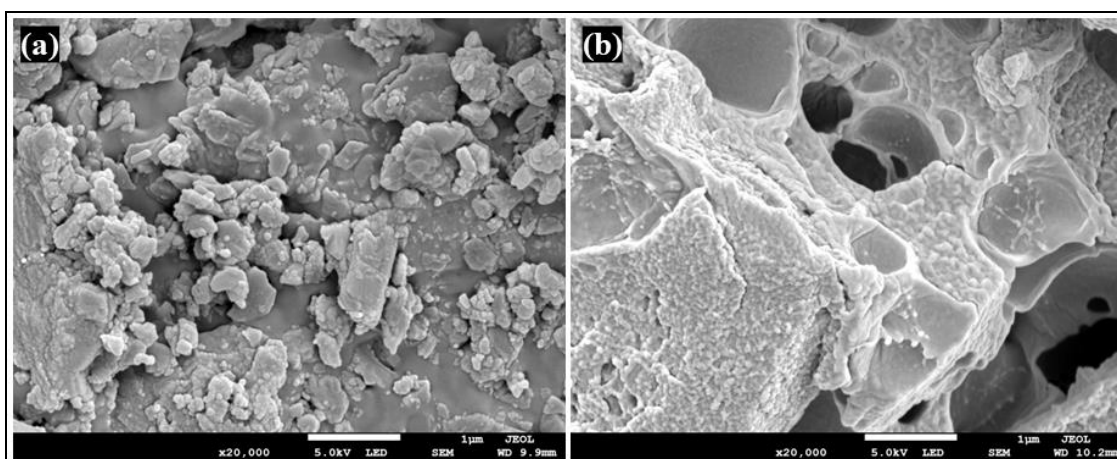


Figure 3.2. FESEM images for (a) WPP and (b) HC/WPP/0.05 at 20,000X magnification.

3.3.3.4. TGA and DTG

The thermal stability of WPP, HC, HC/WPP/0.05 and HC/WPP/NPK was investigated by comparing their weight loss (%). The corresponding TGA and DTG curves are shown in **Figure 3.3.(a and b)**, respectively. The TGA curve of WPP showed two different weight losses corresponding to two peaks in DTG curve. An initial weight loss of approximately 11.6% occurred at temperatures below $143\ ^\circ\text{C}$ and was primarily due to evaporation of retained moisture. The second weight loss starting at $187\ ^\circ\text{C}$ and ending at $308\ ^\circ\text{C}$ was mainly due to thermal decomposition of the C-C polysaccharide chains of cellulosic material [29].

According to the TGA thermograms and DTG curves, the HC, HC/WPP/0.05 and HC/WPP/NPK hydrogels have three major weight loss zones. As shown in **Figure 3.3**, the initial weight loss at temperatures below $240\ ^\circ\text{C}$ is mainly due to the evaporation of retained moisture in HC, HC/WPP/0.05, and HC/WPP/NPK. A second weight loss (%) of the samples in the temperature range of approximately $190\text{--}390\ ^\circ\text{C}$ was mainly due to thermal decomposition of polysaccharide chain. Finally, a third major weight loss occurs

in the temperature range of approximately 350-540 °C. This is due to the breaking of bonds between the grafting monomers and crosslinkers present within the hydrogel network. Finally, the residual weight (%) of HC/WPP/0.05 and HC/WPP/NPK are 43 and 44%, respectively, which are less than the residual weight of WPP (73%), but higher than the residual weight of HC (8%). The highest residual weight in case of HC/WPP/NPK is due to hydrogel loaded by inorganic elements (NPK). Further, from **Figure 3.3.b**, higher initial decomposition temperature for HC/WPP/NPK (347 °C with T_{\max} at 390 °C) was observed compared with HC (226 °C with T_{\max} at 292 °C) and HC/WPP/0.05 (219 °C with T_{\max} at 307 °C), indicating that the former is thermally more stable than the other two samples. However, an exceptionally lower onset degradation temperature for HC/WPP/0.05 was observed which can be ascribed to the formation of its more porous structure [42]. This result is likely due to the incorporation of WPP and NPK into the pure hydrogel structure and the physical cross-linking of the hydrogel composite network [30,31].

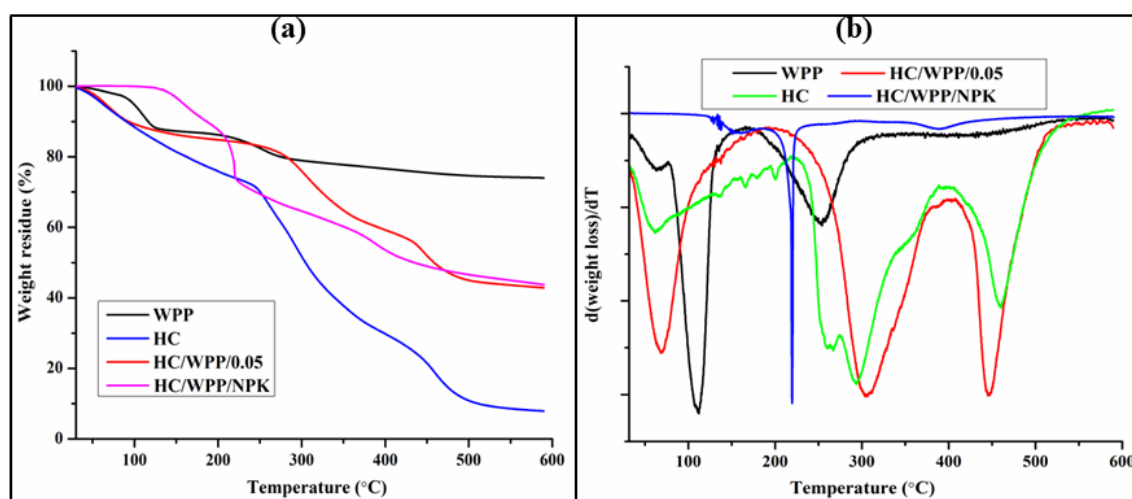


Figure 3.3. (a) TGA thermograms and (b) first derivative of TG curve of WPP, HC, HC/WPP/0.05 and HC/WPP/NPK.

3.3.3.5. Water swelling

The water absorption and water retention capacity of hydrogels are crucial properties for their application in the agricultural field [32]. Therefore, the swelling capacity of the prepared hydrogels were investigated, and the results are shown in **Figure 3.4.a**. HC/WPP/0.05 hydrogel displayed greater WAC of 647 g/g as compared to the neat hydrogel (503 g/g). As can be seen from the figure, the hydrogel showed an increase in water absorption up to 0.05 wt% of WPP content. This phenomenon is attributed to the hydrophilic character of the introduced WPP. WPP introduced hydrogel showed a higher

water absorption capacity compared to pure hydrogel. However, the swelling capacity of the hydrogel decreased from 647 g/g to 219 g/g, when WPP content increased from 0.05 to 10 wt%. The decrease in hydrogel swelling in the presence of more WPP can be attributed to the formation of more crosslinks that restrict the movement of polymer chains [9]. This made it difficult for the network to swell with water, which was the cause of its lower water absorption capacity. Moreover, this is likely due to increased intramolecular bonding between hydroxyl (-OH) groups which in turn results in less hydrophilic -OH groups available for water absorption with increasing WPP content in the hydrogel [32].

As hydrogels with high WAC are highly expandable for agricultural applications as they can gradually release entrapped nutrients along with absorbed water into the soil over a long period of time, which improves RL and SL as well as seed germination rate, etc. [3,33]. Therefore, NPK loaded with HC/WPP/0.05, showing maximum WAC, was selected for fertilizer release and seed germination tests in this study.

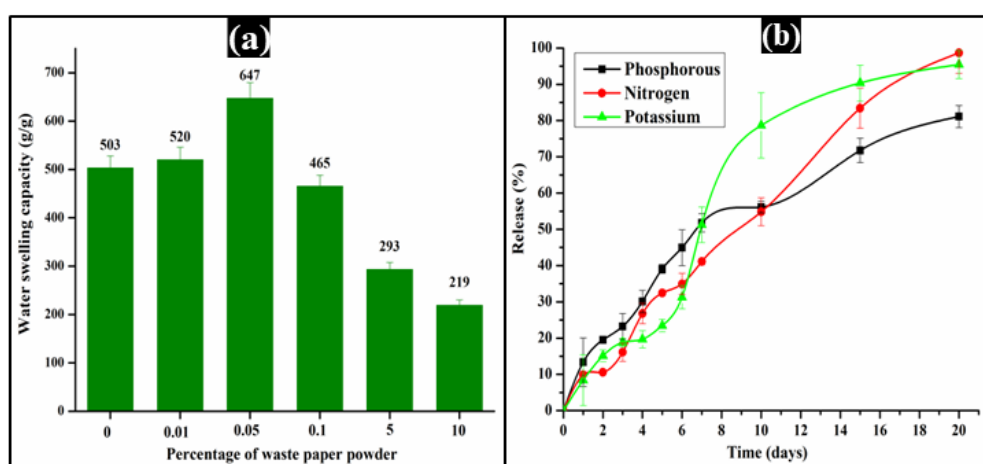


Figure 3.4. (a) Effect of WPP on water absorption capacity of prepared hydrogel composites and (b) NPK release profile of HC/WPP/NPK.

3.3.3.6. NPK release

The slow release of fertilizer is one of the most significant characteristics of SRF system ensuring high nutrient absorption and minimizing nutrient loss [22]. Therefore, HC/WPP/NPK sustained release experiments were performed to evaluate the fertilizer release process. In this study, a mixed mineral fertilizer i.e., NPK containing equal amounts of water-soluble macronutrients like N, P, and K were used. **Figure 3.4.b** illustrates the NPK release profile of hydrogel HC/WPP/NPK for twenty days in water at room temperature. The curves show that the release rates for all three elements were

gradually increased. As seen from **Figure 3.4.b**, HC/WPP/NPK released 13, 9 and 8% of P, N and K, respectively, which did not exceed 15% within first day of incubation and released 81, 98 and 95% of P, N and K, respectively after twentieth day, indicating its good slow-release property [15]. This could be ascribed to the formation of a more cross-linked network structure in the HC/WPP/NPK formulation due to the incorporation of WPP. On the other hand, the intermolecular hydrogen-bonding formed between the hydroxyl groups of WPP, and the functional groups of the polymer matrix retard the dissolution and diffusion of the charged nutrients and slowing down the fertilizer release rate. Besides, cationic and anionic NPK ingredients such as phosphate (PO_4^{3-}), potassium (K^+) and ammonium (NH_4^+) ions can interact via hydrogen and covalent bonds with anionic site present on the surface and within the pores of the hydrogel matrix resulting in the slow-release behavior of the formulation [34]. These results demonstrate the excellent sustained release behavior of the developed formulations and demonstrate the potential for controlled nutrient delivery systems.

3.3.3.7. Kinetic study of NPK release

To analyze the fertilizer release mechanism, we have performed different kinetics models as shown in **Figure 3.5.(a-d)**. Different parameters related to the kinetics models such as release component (n) and the correlation factor (R^2) are summarized in **Table 3.2**. From these data various physicochemical factors affecting the controlled release ability of the hydrogel can be analyzed. According to Korsmeyer–Peppas models if the value of n is < 0.45 refers the Fickian diffusion and in between 0.45-0.89 corresponds to non-Fickian transport. Moreover, if the value >0.89 , then indicates case II transport fertilizer release mechanism. In our study, it is found that the release study follows non-Fickian diffusion, where both swelling and diffusion effect the release phenomenon [35,36].

3.3.3.8. Biodegradation (soil burial method)

The degradation properties of the polymeric material are crucial factors in designing SRF for agricultural applications with minimal environmental impact [37]. The degradation rate is highly dependent on various factors that affecting microbial growth, such as mineral nutrient supply, oxygen concentration, pH, temperature, and humidity [38]. Hence, a biodegradability test of the prepared HC/WPP/NPK hydrogel was performed using the soil burial method. The degradation of HC/WPP/NPK hydrogel in soil at

Chapter 3

ambient temperature over time is presented in **Figure 3.6.a**. The hydrogel's biodegradability was found to be excellent and increased with time, with the highest rate of degradation occurring in the initial days. Decomposition rate after 15 days of soil burial test for HC/WPP/NPK was calculated to be 24%. After 75 days of degradation, the percentage of decomposition was found to be 62%.

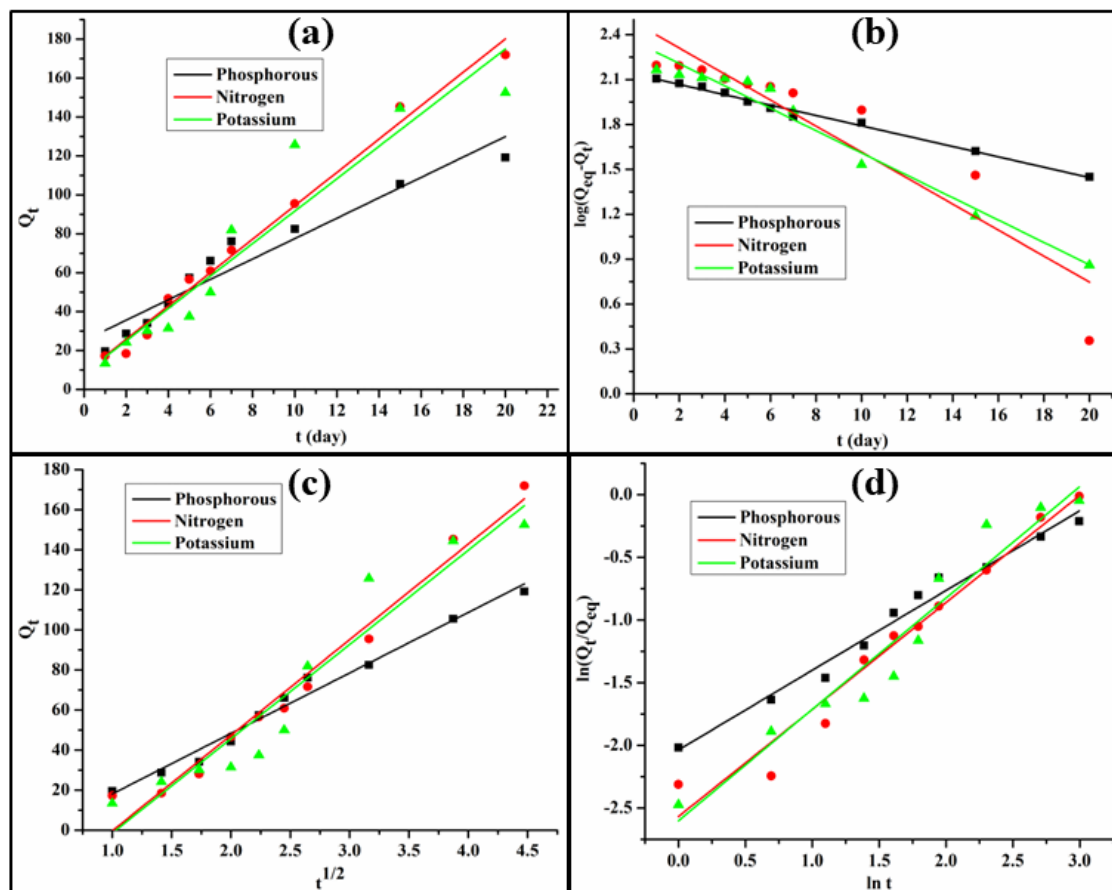


Figure 3.5. (a) Zero order, (b) pseudo-first-order, (c) Higuchi square root law and (d) Korsmeyer and Peppas kinetic plots of NPK release for HC/WPP/NPK.

Table 3.2. Kinetic parameters of several models for NPK release data.

Kinetic model	Correlation coefficient (R^2)		
	P	N	K
Korsmeyer	0.97	0.96	0.93
Higuchi	0.98	0.97	0.91
First order	0.99	0.84	0.96
Zero order	0.92	0.98	0.89
n	0.63	0.85	0.88

Further, the FTIR spectrum and morphology in **Figure 3.6.(b-d)**, demonstrates the chemical structural change (biodegradation) that occurred during the 75 days soil burial test for the HC/WPP/NPK hydrogel. In the FTIR spectrum of HC/WPP/NPK after 75 days of degradation, intensities of some of the peaks have been found to be decreased. Microbial attack in the soil produced these changes in peak positions, signaling the breakage of covalent bonds between polymeric chains [38]. The broadening of the peak at 3434 cm^{-1} for the O-H stretching and the intensity of the peak at 2929 cm^{-1} for the aliphatic C-H stretching decreased upon biodegradation. This indicates cleavage of O-H and C-H bonds by the microorganism during the test. In the degraded hydrogels, the carbonyl peaks (C=O) of the carboxylate groups of AA and IA at 1709 cm^{-1} appeared with a low intensity peak. This indicates the breakdown of the structure of the hydrogel network. Furthermore, the strength of the C-O-C stretching at 1022 cm^{-1} also decreased due to degradation during the soil burial test [39].

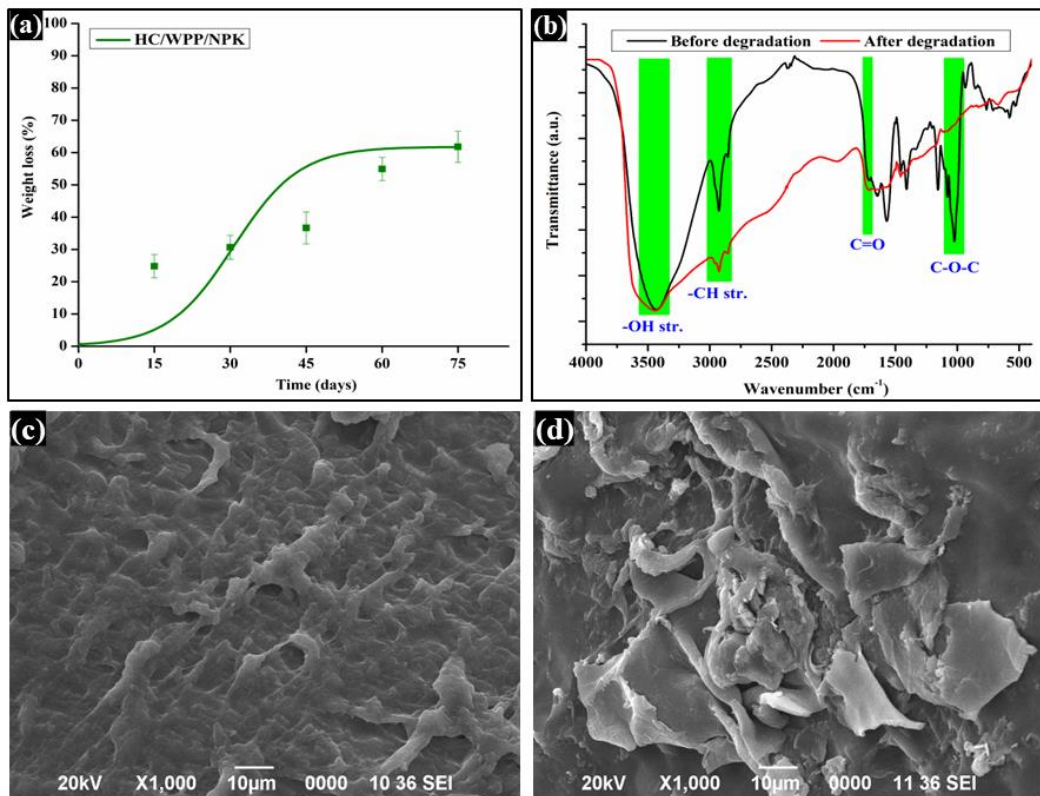


Figure 3.6. (a) Weight loss with time in biodegradation, (b) FTIR spectra before and after degradation; and SEM images of HC/WPP/NPK (c) before and (d) after degradation at 1000X magnification.

Moreover, significant changes in structural morphology were observed after 75 days of the test, and significant degradation of the hydrogel sample was observed. Before biodegradation, the surface of the hydrogel was smooth, as shown in **Figure 3.6.c**. After

biodegradation, SEM image showed the presence of small voids, increased surface roughness and cracks on the surface of the hydrogel (**Figure 3.6.d.**).

Thus, the degradation process showed that the synthesized hydrogel possessed excellent biodegradable property and has no negative impact on the environment and thus can be safely employed for agricultural applications.

3.3.3.9. Effect of HC/WPP/NPK on okra seed germination

In order to explain the effect of HC/WPP/NPK hydrogel, germination-study was conducted on okra seeds. The test was evaluated by measuring the change in RL, SL and the number of germinated seeds planted in both loam soil and sandy soil with hydrogels containing NPK and without NPK. The results are provided in **Table 3.3**. The plant growth after soil treated with two different hydrogels was observed for one week, and the corresponding digital photographs are shown in **Figure 3.7**. Adequate supply of nutrients with water has a significant impact on plant growth, so there was a clear difference in the growth of the studied plants between the treated and untreated soils. The average seedling lengths of okra seeds treated with the hydrogels were significantly larger than the two control groups.

Table 3.3. Effect of HC/WPP/NPK on the growth of okra seeds.

Soil type	Measurement	Control-1	Control-2	HC/WPP/NPK
	Germination rate (%)	-	80	100
Loam soil	Root length (cm)	-	3.16±1.6	6.35±2.4
	Shoot length (cm)	-	8.33±6.82	9.65±1.6
Sandy soil	Germination rate (%)	25	50	75

In loam soil

As shown in **Figure 3.7.(a-c)**, germination count for HC/WPP/NPK was dramatically faster and higher than those for the control-1 and control-2. In the case of control-2 and HC/WPP/NPK, 80 and 100% of germination rate was observed. However, no seed was germinated for control-1 for 7 days of the test. Furthermore, as shown in **Table 3.3**, we found a significant increase in RL and SL of HC/WPP/NPK after 4 and 7 days of germination. The highest RL and SL on 7 days of germination were 6.35 cm and 9.65 cm for HC/WPP/NPK. These results can be attributed to the presence of N, P and K in the

hydrogel structure in the case of HC/WPP/NPK samples, which are the essential macronutrients for plant growth. Further, HC/WPP/NPK can slowly release the absorb water to the soil and plant root through a diffusion driven mechanism. Thus, controlled and sustained release of N, P, K and water from HC/WPP/NPK assisted in germination of seeds and growth of the plants without the need of external irrigations [40]. Moreover, measurements of the germination rate, RL and SL for control-2 showed that the soil treated with HC/WPP/0.05 hydrogels promoted development of okra seeds even if it contains only free hydrogel without NPK. This is likely because HC/WPP/0.05 supplies absorbed water to promote plant growth. However, soil treated without any hydrogel (in case of control-1), cannot supply sufficient water that required for seeds to be germinated. Therefore, no seed germination was observed in that case.

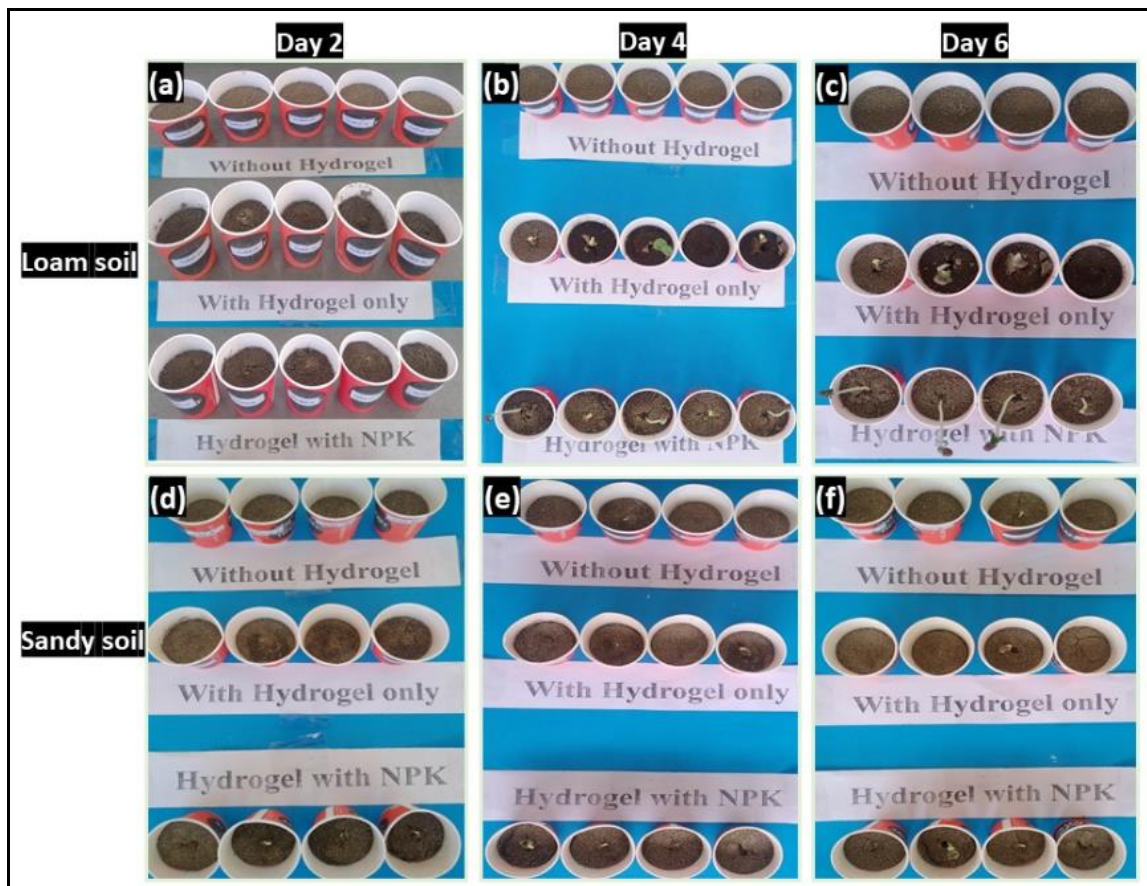


Figure 3.7. Photographs of okra seeds germination after 2, 4, 6 days in loam soil (a, b, and c) and sandy soil (d, e, and f).

In sandy soil

However, a slower seed germination rate was observed for each condition in sandy soil compared to loam soil. After 7 days of seedling, the highest germination rate was observed in the case of HC/WPP/NPK i.e., 75% and no growth of RL and SL was

observed even for HC/WPP/NPK (**Figure 3.7.(d-f)**). This may be due to sandy soils, where water-swollen hydrogels tend to dry out, and unable to maintain soil moisture levels for control release of NPK fertilizer to assist in germination of the seeds. Therefore, we can conclude that the NPK-loaded hydrogel i.e., HC/WPP/0.05 has the potential for applications in agriculture, especially for the growth of okra seeds in loam soil.

3.4. Conclusion

In this work, cellulosic WPP was produced from wastepaper materials and used subsequently as a modifying agent in starch/IA/AA hydrogel matrix to prepare a bio-based hydrogel composite using free radical polymerization method. The structure and morphology of the prepared WPP and hydrogel composite was analyzed using various spectroscopic and microscopic techniques. Further, the maximum WAC of the prepared hydrogel composite was found to be 647 g/g for 0.05 wt% of WPP. Additionally, NPK release and seed germination studies were performed for hydrogel containing 0.05 wt% WPP. It was observed that the hydrogel showed excellent sustain-release ability and has significant effect on the germination rate of okra seeds. Moreover, the results of soil burial test showed the good biodegradability of the hydrogel which confirmed that it has no harmful effect on the environment. Thus, it can be used as potential material for agricultural application as a SRF system.

References

- [1] Nayan, N. H. M., Hamzah, M. S. A., Tahir, A. A. H. M., Rajali, A. A. A., Muslih, E. F., and Mazlan, R. Development of poly(vinyl alcohol)/chitosan hydrogel loaded with fertilizer compound: Preparation, properties and effect on seed germination. *Journal of Science and Technology*, 10(4):21-27, 2018.
- [2] Hanna, D. H., Lotfy, V. F., Basta, A. H., and Saad, G. R. Comparative evaluation for controlling release of niacin from protein- and cellulose-chitosan based hydrogels. *International Journal of Biological Macromolecules*, 150:228-237, 2020.
- [3] Ramli, R. A. Slow-release fertilizer hydrogels: A review. *Polymer Chemistry*, 10(45):6073-6090, 2019.
- [4] Salimi, M., Motamedi, E., Motesharezadeh, B., Hosseini, H. M., and Alikhani, H. A. Starch-g-poly(acrylic acid-co-acrylamide) composites reinforced with natural

- char nanoparticles toward environmentally benign slow-release urea fertilizers. *Journal of Environmental Chemical Engineering*, 8(3):103765, 2020.
- [5] Lotfy, V. F., Hassan, S. S., Khalf-Alla, P. A., and Basta, A. H. The role of side chain of amino acid on performance of their conjugates with carboxymethyl cellulose and their Pd(II) complexes as bioactive agents. *International Journal of Polymeric Materials and Polymeric Biomaterials*, 69(1):21-31, 2020.
- [6] Bauli, C. R., Lima, G. F., de Souza, A. G., Ferreira, R. R., and Rosa, D. S. Eco-friendly carboxymethyl cellulose hydrogels filled with nanocellulose or nanoclays for agriculture applications as soil conditioning and nutrient carrier and their impact on cucumber growing. *Colloids and Surfaces A: Physicochemical and Engineering Aspects*, 623:126771, 2021.
- [7] Wu, Y., Brickler, C., Li, S., and Chen, G. Synthesis of microwave-mediated biochar-hydrogel composites for enhanced water absorbency and nitrogen release. *Polymer Testing*, 93:106996, 2021.
- [8] Das, S. K. and Ghosh, G. K. Hydrogel-biochar composite for agricultural applications and controlled release fertilizer: A step towards pollution free environment. *Energy*, 242:122977, 2020.
- [9] Saini, A., Yadav, C., Bera, M., Gupta, P., and Maji, P. K. Maleic anhydride grafted linear low-density polyethylene/waste paper powder composites with superior mechanical behavior. *Journal of Applied Polymer Science*, 134(31):45167, 2017.
- [10] Lotfy, V. F. and Basta, A. H. Optimizing the chitosan-cellulose based drug delivery system for controlling the ciprofloxacin release versus organic/inorganic crosslinker, characterization and kinetic study. *International Journal of Biological Macromolecules*, 165:1496-1506, 2020.
- [11] De Adhikari, A., Oraon, R., Tiwari, S. K., Lee, J. H., and Nayak, G. C. Effect of waste cellulose fibres on the charge storage capacity of polypyrrole and graphene/polypyrrole electrodes for supercapacitor application. *RSC Advances*, 5(35):27347-27355, 2015.
- [12] Ghosh, R., Mondal, S., Mukherjee, D., Adhikari, A., Ahmed, S. A., Alsantali, R. I., Khder, A. S., Altass, H. M., Moussa, Z., Das, R., and Bhattacharyya, M. Oral drug delivery using a polymeric nanocarrier: Chitosan nanoparticles in the delivery of rifampicin. *Materials Advances*, 3(11):4622-4628, 2022.
- [13] Danial, W. H., Majid, Z. A., Muhid, M. N. M., Triwahyono, S., Bakar, M. B., and

- Ramli, Z. The reuse of wastepaper for the extraction of cellulose nanocrystals. *Carbohydrate Polymers*, 118:165-169, 2015.
- [14] Rana, A. K., Frollini, E., and Thakur, V. K. Cellulose nanocrystals: Pretreatments, preparation strategies, and surface functionalization. *International Journal of Biological Macromolecules*, 182:1554-1581, 2021.
- [15] Pang, L., Gao, Z., Feng, H., Wang, S., and Wang, Q. Cellulose based materials for controlled release formulations of agrochemicals: A review of modifications and applications. *Journal of Controlled Release*, 316:105-115, 2019.
- [16] Hou, X., Pan, Y., Xiao, H., and Liu, J. Controlled release of agrochemicals using pH and redox dual-responsive cellulose nanogels. *Journal of Agricultural and Food Chemistry*, 67(24):6700-6707, 2019.
- [17] Sarmah, D., Borah, M., Mandal, M., and Karak, N. Swelling induced mechanically tough starch–agar-based hydrogel as a control release drug vehicle for wound dressing applications. *Journal of Materials Chemistry B*, 11(13):2927-2936, 2023.
- [18] Mansora, A. M., Lima, J. S., Anib, F. N., Hashima, H., and Hoa, W. S. Characteristics of cellulose, hemicellulose and lignin of MD2 pineapple biomass. *Chemical Engineering Transactions*, 72(1):79-84, 2019.
- [19] de Souza, A. G., Rocha, D. B., Kano, F. S., and dos Santos Rosa, D. Valorization of industrial paper waste by isolating cellulose nanostructures with different pretreatment methods. *Resources, Conservation and Recycling*, 143:133-142, 2019.
- [20] Korostynska, O., Mason, A., and Al-Shamma, A. Monitoring of nitrates and phosphates in wastewater: current technologies and further challenges. *International Journal on Smart Sensing and Intelligent Systems*, 5(1):149, 2022.
- [21] Albuquerque, A. C., Rodrigues, J. S., de Freitas, A. S., Machado, G. T., and Botaro, V. R. Renewable source hydrogel as a substrate of controlled release of NPK fertilizers for sustainable management of *Eucalyptus urograndis*: Field Study. *ACS Agricultural Science and Technology*, 2(6):1251-1260, 2022.
- [22] Rodrigues Sousa, H., Lima, I. S., Neris, L. M. L., Silva, A. S., Santos Nascimento, A. M. S., Araújo, F. P., Ratke, R. F., Silva, D. A., Osajima, J. A., Bezerra, L. R., and Silva-Filho, E. C. Superabsorbent hydrogels based to poly(acrylamide)/cashew tree gum for the controlled release of water and plant

- nutrients. *Molecules*, 26(9):2680, 2021.
- [23] Olad, A., Gharekhani, H., Mirmohseni, A., and Bybordi, A. Superabsorbent nanocomposite based on maize bran with integration of water-retaining and slow-release NPK fertilizer. *Advances in Polymer Technology*, 37(6):1682-1694, 2018.
- [24] Choi, H., Park, J., and Lee, J. Sustainable bio-based superabsorbent polymer: Poly(itaconic acid) with superior swelling properties. *ACS Applied Polymer Materials*, 4(6):4098-4108, 2022.
- [25] Ablouh, E. H., Brouillette, F., Taourirte, M., Sehaqui, H., El Achaby, M., and Belfkira, A. A highly efficient chemical approach to producing green phosphorylated cellulosic macromolecules. *RSC Advances*, 11(39):24206-24216, 2021.
- [26] Baghbadorani, N. B., Behzad, T., Etesami, N., and Heidarian, P. Removal of Cu^{2+} ions by cellulose nanofibers-assisted starch-g-poly(acrylic acid) superadsorbent hydrogels. *Composites Part B: Engineering*, 176:107084, 2019.
- [27] Gharekhani, H., Olad, A., and Hosseinzadeh, F. Iron/NPK agrochemical formulation from superabsorbent nanocomposite based on maize bran and montmorillonite with functions of water uptake and slow-release fertilizer. *New Journal of Chemistry*, 42(16):13899-13914, 2018.
- [28] Dai, H. and Huang, H. Enhanced swelling and responsive properties of pineapple peel carboxymethyl cellulose-g-poly(acrylic acid-co-acrylamide) superabsorbent hydrogel by the introduction of carclazyte. *Journal of Agricultural and Food Chemistry*, 65(3):565-574, 2017.
- [29] Czarnecka, E. and Nowaczyk, J. Semi-Natural superabsorbents-based on Starch-g-poly(acrylic acid): Modification, synthesis and application. *Polymers*, 12(8):1794, 2020.
- [30] Hanna, D. H. and Saad, G. R. Encapsulation of ciprofloxacin within modified xanthan gum-chitosan based hydrogel for drug delivery. *Bioorganic Chemistry*, 84:115-124, 2019.
- [31] Thombare, N., Mishra, S., Shinde, R., Siddiqui, M. Z., and Jha, U. Guar gum-based hydrogel as controlled micronutrient delivery system: Mechanism and kinetics of boron release for agricultural applications. *Biopolymers*, 112(3):e23418, 2021.
- [32] Das, D., Bhattacharjee, S., and Bhaladhare, S. Preparation of cellulose hydrogels

- and hydrogel nanocomposites reinforced by crystalline cellulose nanofibers (CNFs) as a water reservoir for agriculture use. *ACS Applied Polymer Materials*, 5(4):2895-2904, 2023.
- [33] Abobatta, W. Impact of hydrogel polymer in agricultural sector. *Advances in Agriculture and Environmental Science*, 1:59-64, 2018.
- [34] Liu, S., Wu, Q., Sun, X., Yue, Y., Tubana, B., Yang, R., and Cheng, H. N. Novel alginate-cellulose nanofiber-poly(vinyl alcohol) hydrogels for carrying and delivering nitrogen, phosphorus and potassium chemicals. *International Journal of Biological Macromolecules*, 172:330-340, 2021.
- [35] Baruah, M., Borgohain, A., Gogoi, R., Borah, N., Deka, D., Karak, T., and Saikia, J. Optimization of phosphorus-loaded Ni-ZnO cross-linked carboxy methyl cellulose-based biodegradable nanocomposite hydrogel beads for the slow release of P, Ni and Zn: A kinetic approach. *New Journal of Chemistry*, 47(17):8200-8213, 2023.
- [36] Siepmann, J. and Peppas, N. A. Higuchi equation: Derivation, applications, use and misuse. *International Journal of Pharmaceutics*, 418(1):6-12, 2011.
- [37] Tanan, W., Panichpakdee, J., Suwanakood, P., and Saengsuwan, S. Biodegradable hydrogels of cassava starch-g-poly(acrylic acid)/natural rubber/poly(vinyl alcohol) as environmentally friendly and highly efficient coating material for slow-release urea fertilizers. *Journal of Industrial and Engineering Chemistry*, 101:237-252, 2021.
- [38] Choudhary, S., Sharma, K., Bhatti, M. S., Sharma, V., and Kumar, V. DOE-based synthesis of gellan gum-acrylic acid-based biodegradable hydrogels: Screening of significant process variables and in situ field studies. *RSC Advances*, 12(8):4780-4794, 2022.
- [39] Bhaladhare, S. and Das, D. Cellulose: A fascinating biopolymer for hydrogel synthesis. *Journal of Materials Chemistry B*, 10(12):1923-1945, 2022.
- [40] Demitri, C., Scalera, F., Madaghiele, M., Sannino, A., and Maffezzoli, A. Potential of cellulose-based superabsorbent hydrogels as water reservoir in agriculture. *International Journal of Polymer Science*, 435073, 2013.